EFDA–JET–PR(08)58

P.T. Lang, K. Lackner, B. Alper, K. Gál, J. Hobirk, A. Kallenbach, S. Kálvin, G. Kocsis, M. Maraschek, C.P. Perez von Thun, W. Suttrop, T. Szepesi, R. Wenninger, H. Zohm, ASDEX Upgrade Team and JET EFDA contributors

Investigation of Pellet Triggered MHD Events in ASDEX Upgrade and JET

Investigation of Pellet Triggered MHD Events in ASDEX Upgrade and JET

P.T. Lang[1], K. Lackner[1], B. Alper[2], K. Gál[3], J. Hobirk[1], A. Kallenbach[1], S. Kálvin[3], G. Kocsis[3], M. Maraschek[1], C.P. Perez von Thun[1], W. Suttrop[1], T. Szepesi[3], R. Wenninger[1], H. Zohm[1], ASDEX Upgrade Team and JET EFDA contributors*

JET-EFDA, Culham Science Centre, OX14 3DB, Abingdon, UK

[1]Max-Planck-Institut fnur Plasmaphysik, EURATOM Association, Boltzmannstr. 2, 85748 Garching, Germany
[2]EURATOM-UKAEA Fusion Association, Culham Science Centre, OX14 3DB, Abingdon, OXON, UK
[3]KFKI Research Institute for Particle and Nuclear Physics, EURATOM Association, P.O. Box 49, H-1525 Budapest-114, Hungary
** See annex of F. Romanelli et al, "Overview of JET Results", (Proc. 22 [nd] IAEA Fusion Energy Conference, Geneva, Switzerland (2008)).*

Preprint of Paper to be submitted for publication in
Nuclear Fusion

ABSTRACT

To get deeper insight into the MHD activity triggered by pellets we extended our previous analyses of standard type-I ELMs to pellets injected into discharge phases of the following types: Ohmic, L-mode, type-III ELMy H-mode, ELM-free, radiative edge scenarios with type-I ELMs, the Quiescent H (QH)-mode regime. We re-examined also core mode activity like neoclassical tearing modes or snakes. Data were taken from ASDEX Upgrade and JET. It turned out that pellet injection generally creates a strong, local perturbation of the MHD equilibrium in the ablation region and even beyond. Regarding the triggering of ELMs, this initial perturbation can damp out, indicating that the plasma is stable in the corresponding regime even for finite-size perturbations. This behaviour is observed not only in Ohmic and L-Mode phases but also in the QH-mode where the Edge Harmonic Oscillations (EHO) appear to keep the edge in a stable regime. In case the plasma is prone to ELM growth, the large amplitude of the pellet perturbation can trigger the event even in situations where modes appear to be still linearly stable. The non-linear character of the ELM trigger process is highlighted also by the subsequent explosive growth of these events. For edge plasma conditions characterised by higher resistivity the growth time of spontaneously occurring ELMs increases when the plasma changes from the type-I into the type-III regime. Pellet-triggered ELMs, however, maintain the fast rise times otherwise typical for the hot edge type-I regime. Pellet triggering of mode activity can be shown to be a quite universal phenomenon, which, however, only for the case of ELMs can be unambiguously attributed to prompt direct excitation by the pellet.

1. INTRODUCTION

Edge Localised Mode (ELM) induced erosion of plasma facing materials has been recognised as a possible threat to the viability of ITER [1]. Several approaches to solve this problem are currently under investigation. One possible option is to establish ELM control via the pacing concept, by raising, in a controlled manner the ELM occurrence frequency, f_{ELM}, above its natural value, f^0_{ELM}, thereby reducing the energy per ELM ΔW_{ELM} according to the empirically observed relation $f_{ELM} \times \Delta W_{ELM} = \text{const}$: [2]. ELM pacing by the injection of small pellets has been demonstrated successfully over a broad parameter range. Scenarios with controlled ELMs can satisfy even such diverse requirements as impurity expulsion (during intrinsically ELM-free phases) on one, and the reduction of impulsive divertor heat loads on the other hand [3]. To gain insight into the more detailed physics of ELM triggering (and ultimately also into its scaling), we have analyzed pellet injection into different types of discharges. We tested the hypothesis that an injected pellet excites always a helical perturbation, partly by the local interruption of the helical equilibrium current in the edge zone, and partly by the localized change (increase) in plasma pressure. Depending on the stability properties of the pre-injection plasma this excitation should either result in damped oscillations (like the ringing of a chord) or a growing perturbation.

Results of such experiments during Ohmic (OH) and L-mode plasmas as well as in ELM-free, type-III and type-I ELMing and QH-modes confirm this picture. Amongst the investigated scenarios

we included also two in which an enforced enhancement of the edge resistivity resulted in an increased growth time of the spontaneously occurring ELMs. The first stayed in the original type-I regime but with a cooled radiative edge shell established by Argon puffing, the other entered ultimately the type-III regime, driven by edge cooling via enhanced gas puffing. To analyse pellet plasma interaction beyond the impact on edge modes we reconsidered also results regarding the pellet triggering of core MHD modes. Examples chosen here were Neoclassical Tearing Modes (NTM) and the q=1 snake.

Data used in this study are from recent experiments performed on ASDEX Upgrade (AUG) dedicated to ELM triggering but also from previous investigations on AUG and JET using pellet injection for different other purposes (mainly fuelling). The analysis of the latter discharges is partly hampered by the not fully optimized pellet and/or diagnostics settings but the results can nevertheless be used to show the main features of the pellet impact.

2. EXPERIMENTAL SETUP

Most of the analyzed experiments were preformed during the last decade on AUG, a mid-sized divertor tokamak with torus radius R_0 = 1.65m, minor plasma radius a_0 = 0.5m, a typical plasma elongation b/a > 1.6, and a plasma volume V_{Plasma} = 13m^3 [4]. During this period the divertor geometry and the wall material composition have undergone several revisions. The experimental configurations and plasma scenarios of the individual discharges considered are described either briefly in the corresponding sections here or in the documentation of the first analyses of these experiments.

The injector employed is based on a centrifuge pellet accelerator equipped with a storage cryostat pellet reservoir [5]. It is capable of delivering up to 120 cubic pellets of nominal size $(1.4mm)^3$ to $(1.9mm)^3$ (nominal pellet masses m_P corresponding to a particle inventory ranging from 1.6 to 4.1 10^{20} D-atoms) at velocities v_P 240m/s to 1200m/s and repetition rates f_P up to 80Hz. During the period considered, the injection geometry has undergone several modi cations, and the information on the precise version used for a specific experiment can to be found in the references provided.

Diodes detecting the D_α radiation from the plasma region including the pellet path yield a monitor signal for the pellet ablation. To provide knowledge of the pellet position at any time in spite of the possible bending of their trajectories by the ablation process a fast framing camera system has recently been installed [6]. The MHD mode activity in the plasma is monitored by Mirnov coils recording different magnetic field components with high temporal resolution. A set of 30 coils measuring the poloidal magnetic field component on the inner wall of the vacuum vessel covers the entire poloidal circumference. Printed circuit coils measuring the radial magnetic field component are mounted on the magnetic low field side only about 0.1m from the separatrix at different poloidal and toroidal positions. They are particularly suited to study high frequency MHD phenomena like the ELM onset and cycle. Together, covering different poloidal, toroidal and radial positions these diagnostics provide a good overview of the global structure of the MHD perturbation. In addition

to specifically mentioned systems AUG is equipped with a broad range of general diagnostics [4].

Also for JET we re-examined results of earlier experiments dedicated mainly to fuelling. Results from a recent dedicated ELM trigger study on previous JET experiments [7] complemented our data. They cover pellet injection into type-I and ELM-free H-Modes of a large divertor tokamak ($R_0 = 2.96$m, $a_0 = 1.25$m, $V_{Plasma} = 80m^3$). Again, the details of the experimental set up, pellet and plasma parameters can be found in the corresponding references.

3. STRATEGY

To test our hypothesis regarding the crucial role of the pellet-excited helical MHD perturbation for mode destabilisation, we analysed the impact of pellet injection on the mode activity for a broad range of scenarios. Our prime interest was in triggered edge localized modes but to identify more universal features we studied also again the already known impact of pellet injection on core modes. As reference for purely pellet-driven MHD perturbations we used discharges considered immune against spontaneous edge mode activity. Such conditions are expected in plasmas operated well below the L $\rightarrow$ H threshold at low heating power, with little internal energy available to drive instabilities. Gradually increasing heating power and plasma energy makes plasmas more prone to spontaneous but also triggered mode growth. At the same time the evolution of the MHD activity following pellet injection is expected to become dominated less by the onset conditions and more by the growth dynamics of the triggered mode. The systematics of the observed ELM behaviour is dominated by the power flux through the separatrix P_{Sep}. [8] and hence roughly preset by the applied heating power P_H. The studies reported in this paper follow essentially this systematics: For baseline plasma type operation we start with OH discharges as a vehicle to study the pure, directly pellet-induced MHD activity. In this OH regime we investigated the impact of changing the initial pellet perturbation by variation of v_P and/or m_P . L-mode plasmas with moderate auxiliary heating, still regarded stable against ELM activity, were then employed to study the influence of plasma parameters on the pellet induced MHD perturbation.

Crossing the L $\rightarrow$ H transition threshold the plasma enters a regime characterized by a strong transport barrier at the edge resulting in a pedestal with a steep gradient zone. These steep gradients in the plasma pressure and current density profiles are considered responsible for the cyclic appearance of the peeling ballooning instability underlying the periodic ELM events [9, 10, 11]. Following the P_{Sep}. oriented ELM classification [8] for baseline scenarios we enter first the type-III regime ($df_{ELM}/dP_{Sep} < 0$) and reach, with increasing P_{Sep}. finally by $f_{ELM} \rightarrow 0$ the ELM-free regime. Usually, ELM-free phases are not stationary and usable for steady-state operation as e.g. the continuous pro le evolution into an unstable regime and/or impurity accumulation terminate such phases. Proceeding beyond the ELM-free regime to still higher P_{Sep}. results in type-I ELM dominated discharges ($df_{ELM}/dP_{Sep.} > 0$).

Besides these regimes observed generally and reproducibility in baseline scenarios there exist several others plasma regimes - often accessible by applying very special operational conditions -

usually characterized by narrow operational area or limited reproducibility. As an example from this category we report here on the QH mode.

As representative for the pellet impact on core mode activity we re-visited experiments reporting on pellet triggered NTMs, and on pellet-initiated snakes. Different cases will now be discussed in the following.

4. RESULTS

During the investigations, we mainly focussed on the following three issues:

i) what is the magnitude of the local perturbation directly imposed by the pellet,

ii) what are the characteristics of the MHD perturbation directly driven by it,

iii) and what is finally the general response of the plasma MHD evolution.

As a monitor for the first feature we adopt the diode recorded ablation radiation D_α signal. The radiation intensity represents fairly well the time-varying pellet particle ablation rate $dm_P/dt \equiv \dot{m}_P$ [12]; this approximation was well confirmed by our earlier pellet ELM pacing and fuelling studies [13]. All local changes in plasma parameters are ultimately driven by the ablated cold pellet particles and should therefore respond in magnitude to the $\dot{m}_P(t)$ evolution. As indicator for the magnitude of the MHD perturbation we took measurements of $dB_\theta/dt \equiv \dot{B}_\theta$ and $dB_r/dt \equiv \dot{B}_r$ by the Mirnov coils. Our recent investigations on spontaneous and triggered ELMs showed that any of these coils displays the ELM onset fairly well. The first observation of the sharp increase caused by a type-I ELM in the MHD signal is randomly distributed all around the torus and observed within 20s in every coil signal. This was interpreted as result of fast shear Alfven wave communication along magnetic field lines all around the torus of an ELM with an undetermined onset position, also in case of triggered ELMs [14]. To monitor the MHD perturbation we hence either picked a suitable single signal trace or took an average. To characterise the plasma response, and in particular to answer the question whether an ELM was actually triggered, we employed well known indicators like the energy pulse to the strike points visualised by distinct spikes in the divertor D_α radiation or the drop in edge particle and pressure content.

4.1. PURELY PELLET DRIVEN MAGNETIC PERTURBATIONS IN EDGE STABLE REGIMES BELOW THE L → H THRESHOLD

As a first benchmark we tested whether the directly pellet driven perturbation of the magnetic equilibrium is potentially strong enough to explain the ELM trigger. For this we compared the perturbation magnitude of the magnetic geometry at the visible onset of a spontaneous type-I ELM (a triggered one looks virtually identical) to the directly pellet driven perturbation in a regime not prone to ELMs - an OH plasma with low plasma energy. As can be seen clearly in figure 1 the directly pellet driven magnetic perturbation is stronger than that one observed at the time the ELM event can be clearly recognized. It is worth noting that the OH pellet case shown is one of the faintest excitations observed in the study (small 240m/s pellet). The type-I reference discharge

chosen was close in time to it, so as to minimize diagnostic trim di erences. Displayed are (from top to bottom) perturbation monitor signals from $\dot{B}_r$ and $\dot{B}_\theta$ Mirnov coils, D_α pellet and ELM monitor. The latter - like other ELM monitors as well - shows the typical type-I ELM behaviour in the H-mode reference case while clearly no such signature is present in the OH case. The marginal response in the OH case is due to transiently enhanced convective losses after the pellet particle deposition has modified the profiles. When the pellet enters the plasma mode activity sets in (the separatrix crossing was determined from the fast framing camera trajectory reconstruction, details in next section). The magnetic perturbation decays quickly (within about 50s - which is about the same time needed to trigger an ELM after the corresponding perturbation has been imposed [14]) once the driving pellet ablation vanishes after pellet burn out. Hence, it is quite obvious the magnetic perturbation is driven purely by the pellet and no growing mode activity was triggered.

There is a clear correlation between pellet ablation and this directly driven magnetic response. Both displayed Mirnov monitor signals show the same basic trend: an increase in magnitude while the pellet penetrates deeper into the plasma and m_P increases also.

Mounted closer to the separatrix the $\dot{B}_r$ Mirnov coil shows a stronger contribution of higher m,n mode components while the more distant $\dot{B}_\theta$ Mirnov coil is dominated by the slower-decaying low m,n-modes. From this benchmark experiments it is expected that the directly pellet driven magnetic perturbation could trigger an ELM in a suitably unstable plasma. The Mirnov monitor signal can be used to investigate the correlation between the directly pellet driven perturbation m_P and the ultimate plasma response (rapid declining perturbation after pellet burn out or triggering of MHD mode).

To find out if there is a correlation between the pellet imposed perturbation m_P and the directly driven perturbation obviously a regime without significant intrinsic or overlaying triggered MHD activity is required. Thus, in a first exploration we analysed the direct pellet driven impact in a few OH and low power L-mode phases. A dedicated scan comprising 4 discharges was performed launching pellets of different mass and/or velocity into the standard OH discharge (0.8MA, $B_t = -2.5$T) run routinely at AUG plasma operation start up. A few pellets (typically $5-10$ with identical initial m_P and v_P) were injected during the at top phase of each discharge at very low repetition rates (f_P approx. 5Hz) causing only transient perturbations. Hence, all pellets in a single discharge can be regarded as repeatedly performed (virtually) identical experiments.

In different discharges, different pellet velocities (240, 600 or 880m/s), and different pellet sizes - further referred to as small, medium or large - were used (nominal launch m_P due to a particle inventory of 1.7, 2.8 or 4.3×10^{20} D, - however the mass fraction actually arriving at the plasma degrades with increasing speed). The OH reference case shown in figure 1 is taken from this scan.

A simple but robust method was applied to find out if there is a correlation between pellet ablation parameters and the driven MHD perturbations. Initially single characteristic coil signals were compared, while later averaged signals were used. Signals from a dedicated $\dot{B}_r$ Mirnov coil (outboard horizontal mid plane) providing reliable data for all relevant pellets and an ablation monitor showing no indication of saturation were selected. Examples of these signal traces recorded

for two pellets, a large fast and a small slow one, are shown in figure 2.

The Mirnov signal consists mainly of frequency components around 150kHz, around 20kHz and at still lower frequencies. The latter are attributed to plasma pressure profile changes and are not relevant for the present investigation. We therefore filtered them out by using the following simple box car method: For every pellet, the signal was segmented into short time slices (typical 20μs) and the difference between minimum and maximum values in each slice was calculated. The resulting value $\dot{B}_{rp}(t)$ gives the variation in time of the amplitude of the high frequency signal for each pellet, and is in turn modulated by the medium frequency component thought to be caused by the spatial structure of the rotating perturbation and its varying distance to the coil. As the onset of this structure is obviously of statistical nature, we can average all $\dot{B}_{rp}(t)$ for an entire discharge allowing easier comparisons and correlations. The resulting signal $<\dot{B}_{rp}>(t)$ provides then a good measure for the temporal evolution of the magnetic perturbation magnitudes ($<\dot{B}_{rp}>(t)$ corresponds to about 0.7 times the envelope of all single $\dot{B}_{rp}(t)$ curves).

A critical point already for the averaging within one sample but even more for the correlation between different samples is the assignment of time and pellet position. As reference we choose the time of the pellets' separatrix crossing. Identifying this time by the framing-camera-based pellet trajectory reconstruction it is found that the pellet follows straight its designated trajectory without a change in velocity, but also that detectable ablation radiation sets in only once the pellet has penetrated about 10cm beyond the separatrix. This is probably because of the relatively low plasma temperatures in OH discharges. The sensitivity of the visible pellet diagnostics (video observation and photodiodes) is optimised for H-mode discharges in which the formation of the edge pedestal increases the plasma temperature above 500eV at the pedestal top. In such discharges the pellet ablation becomes clearly visible in the edge pedestal, where the plasma temperature is higher than 100eV and increases to 500eV within a few cm. Because of the absence of the edge transport barrier in OH discharges the radial temperature gradient is much smaller and the 500eV is reached only deep in the plasma, typically after the pellet has proceeded about 20–30cm along its path. Taking into account that the pellet ablation rate and hence also the light emission basically scale with $T_e^{5/3}$ (e.g. Neutral Gas Shielding model) it is not surprising that in OH discharges the visible pellet diagnostics will clearly observe the ablating pellet only when the temperature approaches the range of that of the H-mode pedestal, i.e. about 5–10cm inside the separatrix along the pellet path. The onset of MHD activity, on the other hand, coincides well with the instance of separatrix crossing by the pellet, even in the pure OH plasmas when no significant ablation radiation is seen at this moment. Nevertheless the D ablation monitor can still be used as relative measure whose reliability for the subsequent major part of the pellet trajectory was con confirmed by the still observed correlation $\int D_\alpha \sim \int \dot{m}_P \sim \int \tilde{m}_P \sim \Delta N_{plasma}$ ($\tilde{m}_P$ estimated pellet mass arriving in plasma taking into account tube transfer losses [15], ΔN_{plasma} plasma particle inventory enhancement by injection).

An attempt was now made to relate the pellet ablation to the driven MHD perturbation. For a given set of v_P and m_P, $\dot{m}_P(t)$ and $\dot{B}_{rp}(t)$ (or $<\dot{B}_{rp}>(t)$) were found to be well correlated. Changing

of the pellet parameters, however, modifies this correlation: e.g. increasing v_P results in larger values of $<\dot{B}_{rp}>$ (t) for a given $\dot{m}_P$, as is shown in figure 3.

One could argue that what matters is the total amount of particles deposited in a reference volume matters rather than the ablation rate. However, replacing the temporal ablation rate m_P [s^{-1}] by the spatial deposition rate dm_P/dr [m^{-1}] $\equiv m'_P$ (using the relation $m'_P = \dot{m}_P / v_P$) even increases further this mismatch.

Obviously, in the parameter regime investigated pellet particle ablation or deposition rates do not correlate with the resulting magnetic perturbation. As no significant relation of the driven perturbation strength to the underlying pellet born perturbation was found it became clear that the driving mechanism reaches already at every plasma position a saturated regime and the deposition of more pellet particles cannot provoke a stronger Mirnov activity. This implies that there should be still headroom for a reduction of the ablation/deposition rates by injecting smaller/faster pellets while keeping the full drive on the resulting perturbation.

Failing to find a correlation between $< \dot{B}_{rp} >$ (t) and the pellet parameters, we investigated the correlation to local plasma parameters. However, since injection was performed into virtually identical plasmas, data from the pellet parameter scan could only explore the correlation with the pellet penetration into the plasma. The result is shown in figure 4, plotting $< \dot{B}_{rp} >$ evolutions observed for different v_P/m_P samples, versus pellet penetration depths. There is a clear correlation found for all pellet data with an increasing trend with deeper pellet penetration. Obviously only the local plasma parameters are relevant for the magnitude of the pellet triggered perturbation while changes in the ablation/deposition rates imposed under the same local plasma conditions do not have any effect. The reason why larger/faster pellets were found to create a stronger magnetic perturbation lies just in their deeper penetration. For fixed local plasma conditions, however, the same magnetic perturbation is generated by the smallest and largest pellet impacts tested.

For a reasonable interpretation of the pellet induced perturbation of course detailed information on nature and structure of this MHD activity is required. Such information is available from the temporal behaviour of the Mirnov signal frequency power spectrum. An example given in figure 5 shows the frequency amplitude evolution from a Fourier frequency analysis (200s rectangular sliding time window) of a horizontal mid plane LFS Mirnov coil signal. Pellet injection (example shown in right part of figure 2) causes a clearly noticeable event. It consists of a low frequency (up to a few 10kHz) component and toroidicity induced Alfven eigenmode (TAE)-like sub structures in the region between 100 and 200kHz. With toroidal mode numbers ($n \geq 5$) consistent with the Alfven gap structure in OH discharges, the pellet driven MHD activity looks like an enhancement of drift Alfven turbulence driven TAE at the plasma edge in the vicinity of $\rho_{pol} = 0.8$ [16, 17]. With these characteristics the intermediate broad band transient event around 150kHz resemble an ELM pattern [18]. The general temporal frequency behaviour of this intermediate-frequency activity before, during and after pellet ablation is also consistent with an Alfven nature of the MHD activity. Present already weakly before the pellet it is enhanced in amplitude by more than a factor of 100 by the

pellet and than declines rapidly to its initial strength.

To get information on localisation, extent and structure of the pellet enhanced MHD activity, correlation and a mode analysis were performed. A standard cross-spectrum calculation as used in [19] for pairs of magnetic probes made evident the strong correlation caused by the global structure of the mode as shown in figure 6. There, the cross-power spectrum of two Mirnov signals - the one used in the preceding analysis (figure 5) and a second one from another mid plane LFS Mirnov coil displaced by 3 sectors (toroidal distance $3 \times 2\pi/16 \approx 68^{o}$) - is displayed for a time window covering the entire pellet lifetime. The strong correlation in both the low and intermediate frequency ranges during the phase of strong activity indicates a coherent mode. Again we derived toroidal mode numbers of the order 5–6 for the medium frequency components, consistent with TAE activity at the plasma edge. A further, more detailed analysis is under way to identify the connection between this TAE mode close to the edge, excited strongly by the pellet, with the actual seed perturbation in ELM-prone regimes.

Of course data derived from this pellet parameter scan do not allow to differentiate between the influence of different plasma parameters. However, the increase of $< \dot{B}_{rp} >$ with penetration depth seems to indicate that higher local plasma energy densities provide the potential for the excitation of larger MHD perturbations, and suggests that also changes in the plasma conditions would modify the MHD response.

An example further substantiating this claim is shown in figure 7, where applied heating power (with a transiently enhanced Ohmic contribution after pellet injection due to the associated cooling and the increased resistivity), ablation and Mirnov monitor signals are plotted for a train of pellets injected during the L-mode power ramp-down phase before discharge termination. Although subsequent, virtually identical pellets penetrate deeper into the plasma, the resulting pellet born MHD perturbations actually decrease with decreasing energy density. Cleary, lower local plasma energies result in a reduction of the MHD excitation attainable by the pellet perturbation.

The experimental results shown here regarding the directly pellet driven MHD perturbation in edge-stable regimes below the L-H threshold are only a rst step towards the detailed characterisation required for an understanding of the e effects causing the ELM triggering by a pellet. More refined measurements to resolve details of the spatial and temporal structure of the pellet born MHD perturbation and its correlation with pellet parameters are in preparation on AUG and JET.

4.2. PELLET PERTURBATION AS PROBE FOR THE EDGE STABILITY: REGIMES ABOVE THE L → H THRESHOLD

As previously described, we re-investigated recent experiments performed on AUG and JET with respect to the pellet's potential for mode destabilisation in the regimes beyond the L-H threshold. Following the typology described in [8] we discuss rst the type-III regime.

4.2.1 Cold edge, resistive type-III regime

For separatrix heat fluxes just above the L-H threshold tokamak plasmas usually are in the type-III

ELM regime. For operational reasons discharges are often driven at first into the low density type-I ELM regime by a step increase of the heating power, to approach then more gently the type-III regime following a gradual increase of edge cooling. The evolution of such a discharge is shown in the left part of figure 8. Stable strong gas puffing is applied to the steady state type-I ELMy H-mode causing edge cooling and hence an increase of resistivity. This finally results in a transition to the type-III ELM regime; the type-III character is confirmed by the frequency power spectrum of the MHD ELM precursor and the inverted relation between heating power and f_{ELM} [8]. Throughout this transition we performed low frequency injection of rather large pellets. Details of the ELM response to pellet injection for both ELM types are shown on an expanded time scale in the right part of figure 8. During the type-I phase (discussed in detail later), both spontaneous and triggered ELMs show a fast onset, as can be seen from the burst-like MHD signature and the fast-rising D_α radiation from the outer strike point region. It should be noted that the triggered ELM appears to be somewhat enhanced by the large transient particle and energy throughput connected to the pellet ablation - an effect vanishing when the pellet mass is reduced [13]. Spontaneous ELMs in the type-III regime display a significantly slower MHD evolution than in the type-I regime. Triggered ELMs in the type-III regime seem to show a fast type-I ELM like MHD onset (data shown are taken from a twin discharge) while keeping a type-III like divertor heat load pattern. For the type-III ELM case shown here the pellet arrives in a truly quiescent phase between subsequent type-III ELMs. Such a clear separation between triggered and spontaneous ELMs - generally the case in type-I regimes - occurs only rarely in type-III situations, due to their higher natural repetition frequency and the longer duration of the individual events. Nevertheless, results indicate that in the high edge resistivity type-III regime - where spontaneous ELMs are characterized by precursor activity and there for a slow growth -the pellet triggering results in a significantly faster growth by skipping the precursor stage.

4.2.2 The (transient) ELM-free regime

The type-III and the type-I regimes are separated by the ELM-free regime. Its operational window is usually quite narrow and its appearance transient. ELM-free phases are not stationary since e.g. continuous profile evolution and/or impurity accumulation finally terminate these phases. As a consequence, for example, integrated radiative high performance scenarios established at AUG for operation with a full tungsten wall coating of plasma facing components required pellet ELM pacing to keep them in the type-I regime with a sufficiently high f_{ELM} [3]. Otherwise, a too low or vanishing ELM frequency results in a radiative instability leading to short H $\rightarrow$ L back transitions.

Longer lasting but still not steady-state ELM-free phases where observed during investigations performed at JET. Pellet fuelling attempts into hot-ion JET discharges with naturally emerging distinct ELM-free phases showed that every pellet launched caused the appearance of an ELM [20]. A recent detailed re-analysis of JET pellet experiments performed with the explicit aim of ELM triggering [7] confirmed and broadened this finding. An ELM can be triggered any time in an ELMing or ELM-free H-mode phase. Often, the entire ELM behaviour is altered and a train of

ELM follows after pellet injection. This is attributed to the pellets' fuelling impact causing a significant change of plasma parameters and transport characteristics at the edge as a similar behaviour found in AUG [13] could be accounted for by this effect. Again in con rmation of AUG findings, also at JET the initial pellet trigger is found not to be caused by the global fuelling effect but by the prompt local perturbation imposed. The triggered ELM becomes already visible when only a tiny mass fraction (about 1%) is ablated and the pellet is still in the edge barrier region and has not yet changed the global plasma parameters significantly. Thus, all recent investigations showed that the response to pellet injection does not noticeably differ between ELM-free and type-I ELM phases. Hence, with respect to ELM triggering, the ELM-free regime can be considered as type-I phase with a vanishing natural ELM rate.

4.2.3 The standard hot edge type-I ELM regime

The current ITER baseline scenario is the H-mode regime with a hot edge and clear type-I ELMs. In this operational mode the uncontrolled ELMs are expected to cause strong energy bursts whose impact would reduce the divertor lifetime in an unacceptable way [1]. Driven by this concern, most investigations on ELM pacing and pellet triggering of ELMs have been performed in this regime. Following rst pellet ELM pacing and mitigation proof-of-principle experiments also investigations dedicated to the physics of the trigger process were made. To provide stable and robust target plasmas with well separated spontaneous ELM events, such investigations were usually performed in the perturbative limit, where the pellet rate was small compared to the spontaneous ELM repetition frequency and also small enough to avoid any lasting pellet impact on the global plasma parameters. Every pellet therefore probes the response of the unperturbed target plasma in an arbitrary phase of its natural ELM cycle. On account of the practical importance, pellet triggering investigations in the type-I ELM regime are so far the most advanced ones, so that this study can be regarded as an extension of these previous investigations. We therefore recapitulate here just their main results, described in more detail in [14] to put them into the context of a broader view on the pellet triggering of ELMs or MHD activity in general.

Spontaneous ELMs in the hot edge type-I regime show (mentioned before, see fig.8) a rise time as fast as triggered ELMs. For an ensemble of spontaneous ELMs we derived a value of 67 ± 2s for this growth time, for an ensemble of triggered ELMs under identical plasma conditions a virtually identical value of 72 ± 22s. Also, no other significant differences can be observed between triggered and spontaneous ELMs in the MHD dynamics at onset. For small pellets with sufficiently little impact on the discharge fuelling (typically the pellet mass shall not be larger than the ELM induced particle loss of a spontaneous ELM in this regime) we find also no di erences during the later stages in the global appearance, dynamics, duration and spatial distribution of the divertor power flux, if we compare spontaneous and triggered ELMs with the same repetition frequency. Also, the mode and turbulence spectra are quite similar. Essentially, apart from the clearly enforced onset, triggered and spontaneous ELMs are virtually indistinguishable [21, 22].

Specific investigations of the nature and dynamics of the trigger process showed that the pellet-imposed local perturbation triggering the ELM onset is imposed in the centre of the edge transport barrier. A delay is observed between the implementation of the initial local perturbation and the ELM onset of about 50μs - a value coinciding, as already mentioned, with the observed decay time of a purely pellet driven MHD perturbation in OH phases. No significant spatial correlation was found between the pellet injection position and the poloidal or toroidal location at which a first ELM indication was found on a Mirnov coil. The MHD signature of every ELM appears over the entire edge region within about 20s (for reference: fast shear Alfven wave transit time $2\pi R_0/v_A \approx 1$s).

4.2.4 The type-I ELM regime with a radiatively cooled resistive edge

Experiments on controlled edge and hence divertor cooling by Ar seeding were reported in detail in [3] in which transient ELM-free phases were avoided by applying pellet pacing. Whereas usually the pellet pacing frequency sets the ELM frequency, a higher ELM frequency established itself in several of these discharges (f_P about 40Hz, f_{ELM} about 80Hz). In such discharge phases both spontaneous and triggered ELMs occured. As reported in [3], again no significant difference was found between the global action of both ELM types. During the Ar seeding phase a significant reduction of the deposited power density along strike point contours was found. Following Kallenbach's analysis [3], the power load close to the outer strike point was investigated separately for the two kinds of ELMs.. The refined analysis is shown in the left part of figure 9. Triggered and spontaneous ELMs showed an identical behaviour within their individual scatter (boxes representing the 2σ width of an ensemble of ELMs recorded during one stable steady state pacing phase) but a significant reduction in power flux with respect to the reference (non-seeded) type-I ELMs. A striking difference is found, however, in the MHD onset dynamics. This is illustrated by the right part of figure 9, showing for each type both signal traces of typical single events and the values obtained by averaging over the entire ensemble. Whereas the spontaneous ELMs grow significantly slower in the cool edge regime (154 ± 68μs), triggered ones (60 ± 38μs) keep the fast MHD onset observed in the hot edge case. This confirms the observations made in the comparison of triggered and spontaneous ELMs in type-III and hot edge type-I plasmas. In the low resistivity hot edge mode case spontaneous and triggered ELMs evolve equally fast, obviously, as the growth rate of a spontaneous ELM is so large that even the finite-size seed pellet perturbation cannot accelerate the ELM dynamics any further. Increasing edge resistivity results in a reduction of the spontaneous ELM growth rate. In this case, forcing of the ELM by a pellet restores the fastest possible growth leading to a different ELM dynamics.

4.2.5 The quiescent H-mode

The above view on the type-I ELMy H-mode regime concludes the examination of the baseline regimes appearing in a scan of separatrix power flux. It was found that every pellet injected could trigger an ELM, which always showed the fastest evolution observed under any conditions in plasma

discharges of the respective type. Obviously additional information on the pellet perturbation/ELM trigger mechanism from other high confinement regimes, accessible only by changing key discharge parameters (shaping, pumping, divertor configuration, heating configuration, ramp-up scenario ...) would be extremely helpful to get insight in the physics of the trigger process. Unfortunately little information is available as yet for such regimes, with the exception of the QH-mode. The QH mode is a quite interesting regime with respect to edge instabilities and related energy bursts. It displays no strong burst-like transport but the presence of an Edge Harmonic Oscillation (EHO). While the QH regime's very narrow operational range is a clear disadvantage with respect to operational considerations it is nevertheless of great interest to investigate the pellet impact. Results shown here are taken from an experiment aiming to fuel QH plasmas using pellets; details can be found in [23]. For this reason, the pellet size chosen was rather large. The temporal evolution of a discharge showing a transition from type-I to QH without significant changes of global plasma parameters is plotted in the left part of figure 10. A Mirnov monitor signal blow-up at the top shows the EHO with a fundamental frequency of about 10kHz, characteristic for the QH phase. The right part of figure 10, shows a comparison of a spontaneous type-I ELM with the consequences of a pellet impact on a QH discharge. The pellet drives a direct magnetic perturbation like in the sub-H-mode regimes, but - despite its large size - does not trigger an ELM. Consequently, there is also no detectable global energy release as would be expected in case of the triggering of an ELM. The slight erosion of the pedestal is attributed to the observed transport enhancement following from the massive pro le perturbations caused by the pellet injection - an effect well known from pellet fuelling experiments [24]. According to this experiment a pellet cannot trigger an ELM in the QH mode, a regime obviously not providing conditions where the pellet imposed perturbation can seed an instability subsequently growing into a macroscopic MHD perturbation.

4.3. PELLET IMPACT ON CORE MHD ACTIVITY

Edge localized modes are not the only examples of MHD activity that can be triggered by the injection of pellets. To identify possible similarities in the underlying physics processes, we re-visit here also a few examples where pellets are known to have significant impact on core MHD activity. We aimed to distinguish the direct impact localized in three dimensions from effects resulting from the changes in the 1-d profiles of global plasma parameters once a flux surface equilibrium is re-established.

4.3.1. Neoclassical tearing modes at the q = 3/2 surface

NTMs are a known and relatively well understood example of a non-linear instability, which needs a finite size perturbation as trigger. In fact, the triggering of NTMs by pellets was found to reduce the global discharge performance in fuelling studies, but turned out useful for mapping-out their onset requirements by providing a reproducible seed perturbation. A study by Zohm et al. [25] identified, at given magnetic field the onset pressure of m=3,n=2 NTM as a pure function of the

local ion temperature by saw-tooth or pellet created seed islands. For both trigger types, the mode growth lasts several 10 ms. However, as the mode growth is on a transport time scale it does not allow to prove directly the NTM was triggered by the fast action of the imposed local 3D perturbation. Hence triggering of (3,2) NTM by the immediate localized pellet effect cannot be claimed yet.

4.3.2. Snakes at the q = 1 surface

The phenomenon termed snake observed under certain conditions is attributed to the formation of a helical closed-flux-surface region with enhanced confinement usually at the q = 1 surface. Reliable triggering of such snakes was reported for deep pellet penetration in JET [26]. They were also observed in AUG, as shown in figure 11. For the case shown, repetitive pellet injection in an OH discharge caused strong persistent cooling of the plasma leading to successively deeper penetration of the pellets. With the pellets advancing deep into the plasma, pellet ablation and deposition results finally in the occurrence of a helically localised density perturbation. The gradual growth between two pellet events is shown in the left part of the figure displaying the evolution of two adjacent soft x ray (SXR) channels, a tangential Bremsstrahlung view, the line averaged density for the central chord and the pellet monitor signal. Every pellet destroys the previous snake structure but a new one develops until the density rise after several pellets causes a termination of the discharge. The snake structure is located most probably nearby the q = 1 surface (surface location taken from equilibrium reconstruction). It starts with a rotation in the ion diamagnetic drift direction, i.e. opposite to the usual direction of MHD mode rotation in OH discharges [27]. Then the rotation frequency slows down and ultimately reverts to the electron drift direction. For the snake we estimate a final extension as indicated in the right part of figure 11. Covering finally about 2% of the plasma volume, the snake carries an additional particle content of about 5%m̃P increasing the local electron density by about 20%. Again it is yet unproven that a pellet perturbation at the q = 1 surface is a necessary prerequisite as mode growth takes place on the transport time domain of several 10 ms. Pellet triggering of the snake onset confirms NTM results: provided onset conditions of the global plasma parameters are fulfilled a pellet perturbation triggers the event. Although in both cases the initiation of the phenomenon by the prompt local perturbation appears plausible, the slow time-scale of its evolution prevented yet such a clear demonstration like for the ELMs.

DISCUSSION

The investigations made during this study can be applied to check the physics understanding and corresponding models for the origin and the dynamics of ELMs. The occurrence of ELMs is usually attributed to the peeling-ballooning stability boundary touched or transpassed in a region slightly inside the separatrix. Once the mode has become potentially unstable, fluctuations of the local plasma parameters in the region with the highest mode growth rate form the microscopic seed perturbations which evolve into the macroscopic ELM instability that ultimately results in a fast transient collapse of the edge transport barrier. The corresponding losses of pressure, particles etc.

are believed to cause the relaxation of edge parameters back into a stable regime, till radial transport replenishes the edge region to initiate the next ELM cycle. The observation that a strong local perturbation can trigger an ELM at virtually any instant during this cycle contradicts this conventional picture. In ELMing regimes as investigated in this study, the plasma edge must be in a nonlinearly unstable regime at virtually any time of the ELM cycle. This is consistent with a model, where the ELM growth rate depends not only on the background plasma parameters, but also on the instantaneous mode amplitude, like in the well-known paradigm for the NTMs. A strongly non-linear behaviour of edge-localized mode growth rate is found in the calculations of Wilson et al. [28], but might also be the result of more complex interplay between the profiles of pressure, current density and rotation.

Evidently it is also of great practical importance to understand the creation of the seed perturbation by the pellet and to quantify the requirements on its size for initiating an ELM, if we envisage triggering respectively pacing ELMs at a larger size tokamak, and in particular ITER. For this we must know both the physics of pellet ablation and of the ELM trigger. When a deuterium pellet enters the plasma it is exposed to hot energy carriers which erode its surface strongly as the sublimation energy of the hydrogen isotope ice is very low ($\in_{sub} \sim 0.005$eV=particle). Accordingly a spherically expanding neutral cloud forms around the pellet [29], which gradually becomes ionized. In this latter stage the cross field expansion of the cloud is stopped and the plasmoid is stretching out along the field lines [30, 31]. The bright, luminescent part of the plasmoid characterized by its D_α radiation has an extension along field in the order of 10cm [32]. At its edge, the radiation signal disappears due to the vanishing of the neutral density [6]. Even beyond this visually striking structure observed during the ablation the field aligned cloud expansion continues [33, 34]. This helical structure constitutes a perturbation of the axisymmetric equilibrium, which will relax by the excitation of a broad band of Alfven type waves, damped by dissipation and phase mixing. Except in the singular situation, however, in which the axisymmetric background profiles of the plasma parameters were to pass from a stable to an unstable situation at the nearly exact instance of the pellet injection, these perturbations are unnecessary for the excitation of a linear instability. Of course, the pellet will also modify the axisymmetric profiles of the plasma parameters [35, 36], which might drive the latter over the brink of the linear stability threshold. Again, however, this e effect would very strongly depend on the natural proximity of the plasma to the threshold - and hence on the phase of the ELM in which it is hit by the pellet - and also on the size of the pellet. This is again in contradiction with the observation that within the rather broad range of pellet parameters every pellet injected into a type I, type III or ELM-free plasma caused an ELM, irrespective of its phasing with respect to the last ELM-initiated breakdown of the edge barrier. Obviously this general statement has to be qualified, as the sizes, injection velocities and repetition frequencies of the pellets used were still limited to a finite range, and most of the results reported refer to a single tokamak device. Hence the extrapolation of the statement to ITER conditions, and the practicability of pellet pacing on this device are still uncertain. The uncertainties will undoubtedly be diminished by the future pacing

experiments on JET, but will also decrease with the progressing of our understanding.

The evidence presented in this paper concerning the response of robustly ELM-resilient regimes (OH and L-mode plasmas) to the imposed perturbations, and the universality of the triggering process in ELM prone regimes is, however, most consistent with a picture, where potentially ELMing discharges spend most of their time in a non-linearly unstable regime, where any sufficiently large helical perturbation can initiate growth of a perturbation. Evidently such a picture gets support from the calculations of Wilson [28], which describe a mode growth increasing in rate with the growth of the perturbation, although some suppression e effect has still to be identified (differential rotation [37]?) to prevent mode growth from arbitrarily small initial perturbations. The spontaneous growth of intrinsic ELMs in such a model would be understood as the arrival of the plasma profiles in a state where the size of the required trigger perturbation tends practically to zero, so that any statistical fluctuation initiates the breakdown. In this case, the initial mode growth should reflect the behaviour of a linear instability, whereas the finite size perturbation imposed by the pellet would bring the perturbation immediately into a highly non-linear regime. Of particular interest in this context are the observations in the QH-mode[23], which in the frame of our model should correspond to a particular class of plasma profiles (requiring for their attainment also special external measures) where the development into a nonlinearly strongly unstable state is prevented, possibly by the self-regulating action of the observed EHOs. Evidently this hypothesis raises the interest into future experiments with pellet injection into other regimes, like the situation where ELMs are suppressed by the action of resonant magnetic perturbations. The absence of an immediate ELM-trigger by an injected individual pellet in such a case would be taken as a confirmation that the externally imposed field perturbations keep plasma profiles away from non-linearly unstable situations. A delayed reaction would have to be interpreted as the result of the pellet-induced changes in the axisymmetric profiles [38].

A host of future experiments and measurements could support or disprove the above model, by offering more detailed insight in the underlying dynamics. Such kind of information might become available from a better resolution of the temporal and spatial origin of the triggered ELM. Eventually detailed investigations of the observed delay time between ELM onset and imposed pellet perturbations at different poloidal position might help to identify the detailed trigger mechanism. Both the perturbation effect of the pellet and the edge stability characteristics can be sounded out by launching pellets into plasmas in different regimes, but also during phases of active manipulation of the plasma edge e.g. by enhanced ripple [39], edge ergodisation [40, 41] or fast plasma motions [42, 43]. And finally, the impact of pellet pacing on edge profiles and its self- consistent feedback achieving steady state conditions can provide valuable information on the trigger process and its limitations. There are e.g. indications from AUG pacing investigations that while the driven fELM can be imposed instantly, a finite response time is required (in the order of about 100 ms) to achieve actual ELM mitigation and to re-establish the relation $f_{ELM} \times$ ELM = const: [2]. It will also be of interest if and how the ELM triggering behaves when applied over a broader operational space, especially to situations with a larger - and hence more ITER relevant - frequency enhancement

ratio between the driven and spontaneous ELMs.

The questions that have ultimately to be answered are: is successful ELM pacing by pellets possible at ITER and if yes what are the optimized pellets parameters, particularly in view of the fact that the pellet pacing system will make a - possibly unwanted - contribution to refuelling. At present there appears to be quite some headroom available to reduce the associated fuelling contribution, as the imposed MHD perturbations seem to depend on penetration depth but not on the ablation rate. ITER could therefore go for faster pellets to reach the required penetration depth with pellets of sufficiently small mass. Besides reducing energy losses associated with the imposed enhanced convection this could also ease the pumping load, currently a main concern at ITER. Upcoming investigations at AUG with its new re-located blower gun [44], at JET - now equipped with a novel specially tailored injection system [45]- and at DIII-D with the new pellet dropper installed [46] are expected to clarify many of these questions.

REFERENCES

[1]. Federici, G. et al., Plasma Physics Controlled Fusion **45** (2003) 1523.
[2]. Herrmann, A., Plasma Physics Controlled Fusion **44** (2002) 883.
[3]. Kallenbach, A. et al., Journal Nuclear Materials **337-339** (2005) 732.
[4]. ASDEX Upgrade Team, Fusion Science and Technology **44** (2003) 569.
[5]. Andelfinger, C. et al., Review Scientific Instruments **63** (1993) 983.
[6]. Kocsis, G. et al., Review Scientific Instruments **75** (2004) 4754.
[7]. Lang, P.T. et al., Nuclear Fusion **47** (2007) 754.
[8]. Zohm, H., Plasma Physics Controlled Fusion **38** (1996) 105.
[9]. Connor, J.W. et al., Physics of Plasmas **5** (1998) 2687.
[10]. Wilson, H. et al., Nuclear Fusion **40** (2000) 713.
[11]. Snyder, P.B. et al., Plasma Physics Controlled Fusion **46** (2004) A131.
[12]. McNeill, D., J. Nuclear Materials **162-164** (1989) 476.
[13]. Lang, P. T. et al., Nuclear Fusion **43** (2003) 1110.
[14]. Kocsis, G. et al., Nuclear Fusion **47** (2007) 1166.
[15]. Lorenz, A. et al., Fusion Engineering Design **69** (2003) 15.
[16]. Maraschek, M. et al., Physics Review Letters **79** (1997) 4186.
[17]. Scott, B., Plasma Physics Controlled Fusion **39** (1997) 471.
[18]. Bolzonella, T. et al., Plasma Physics Controlled Fusion **46** (2004) A143.
[19]. Strait, E.J. et al., Plasma Physics Controlled Fusion **36** (1994) 1211.
[20]. Alper, B. et al., ELMs, precursors and triggers on JET, in Europhysics Conference Abstracts (CD-ROM,Proc. of the 29thEPS Conference on Plasma Physics and Controlled Fusion, Montreux, 2002), edited by Behm, R. and Varandas, C., volume 26B, page P1.025, Geneva, 2002, EPS.
[21]. Lang, P.T. et al., Nuclear Fusion **44** (2004) 665.
[22]. Neuhauser, J. et al., Nuclear Fusion **48** (2008) 045005.

[23]. Suttrop, W. et al., Nuclear Fusion **45** (2005) 721.
[24]. Lang, P. T. et al., Nuclear Fusion **36** (1996) 1531, Corrigendum in Nucl. Fus. **36** (1996) 153.
[25]. Zohm, H. et al., Nuclear Fusion **41** (2001) 197.
[26]. Wesson, J.A., Plasma Physics Controlled Fusion **37** (1995) A337.
[27]. Klüber, O. et al., Nuclear Fusion **31** (1991) 907.
[28]. Wilson, H. and Cowley, S., Physics Review Letters **92** (2004) 175006.
[29]. Parks, P.B. and Turnbull, R. J., Physics of Fluids **21** (1978) 1735.
[30]. Durst, R. et al., Nuclear Fusion **30** (1990) 3.
[31]. Wurden, G.A. et al., Review Scientific Instruments **61** (1990) 3604.
[32]. Müller, H.W. et al., Nuclear Fusion **42** (2002) 301.
[33]. Kaufmann, M. et al., Nuclear Fusion **26** (1986) 171.
[34]. Lengyel, L.L. et al., Nuclear Fusion **39** (1999) 791.
[35]. Milora, S.L. et al., Nuclear Fusion **35** (1995) 657.
[36]. Pegourie, B., Plasma Physics Controlled Fusion **49** (2007) R87.
[37]. Saarelma, S. et al., Plasma Physics Controlled Fusion **47** (2005) 713.
[38]. Baylor, L. et al., Nuclear Fusion **47** (2007) 1598.
[39]. Saibene, G. et al., Nuclear Fusion **47** (2007) 969.
[40]. Moyer, R.A. et al., Phys. Plasmas **12** (2005) 056119.
[41]. Liang, Y. et al., Physics Review Letters **98** (2007) 265004.
[42]. Degeling, A. et al., Plasma Physics Controlled Fusion **45** (2003) 1637.
[43]. Lang, P.T. et al., Plasma Physics Controlled Fusion **46** (2004) L31.
[44]. Lang, P.T. et al., Review Scientific Instruments **78** (2007) 023504.
[45]. Geraud, A., The JET high frequency pellet injector project, in 24th SOFT Conference, Warsaw, 2006, pages P4-H-201, 2006.
[46]. Baylor, L. et al., Bull. American Physics Society **51**, 115 (2006).

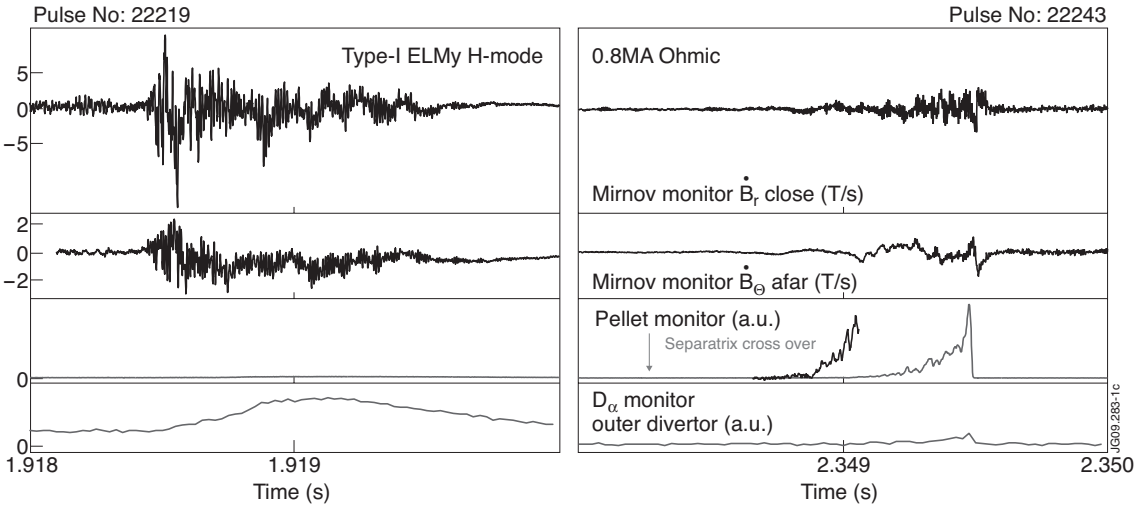

Figure 1: Comparison of a spontaneous type-I ELM and the purely pellet driven MHD perturbation in an OH plasma (identical scales and diagnostics settings). The amplitude of the pellet driven MHD perturbation in the OH case clearly exceeds that one observed as present at the visible ELM onset - despite the fact this OH reference case represents the weakest impact observed over the range of technically available pellet parameters.

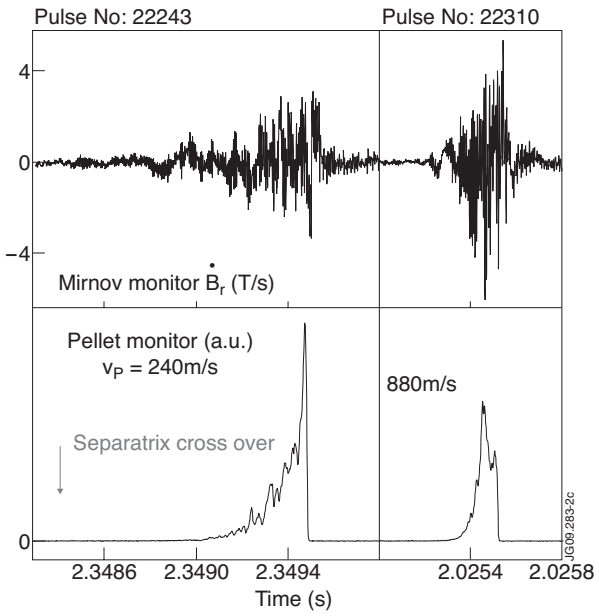

Figure 2: Signal traces representing pellet ablation and resulting MHD perturbation as applied in the analysis for most extreme cases available - a small 240m/s and a large 880m/s pellet.

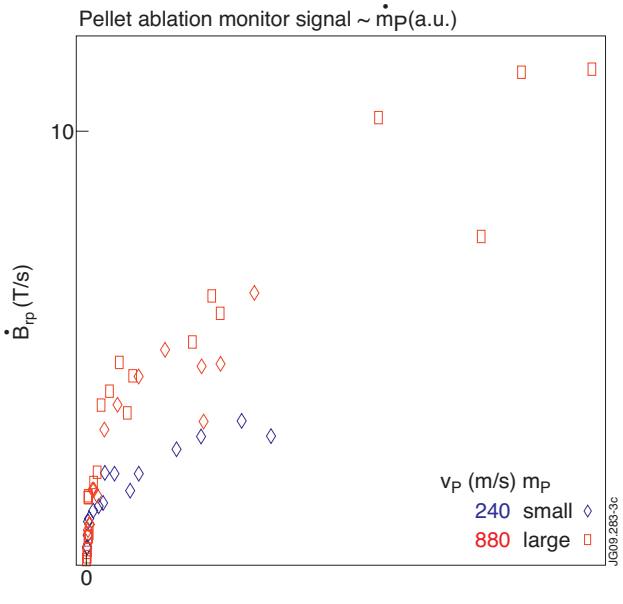

Figure 3: Pellet induced magnetic perturbation $<\dot{B}_{rp}>$ versus pellet ablation rate $\dot{m}_P(t)$ at different pellet speed (240 and 880m/s). Obviously, no correlation between the initial pellet particle deposition and the driven MHD perturbation exists in the investigated regime of pellet parameters.

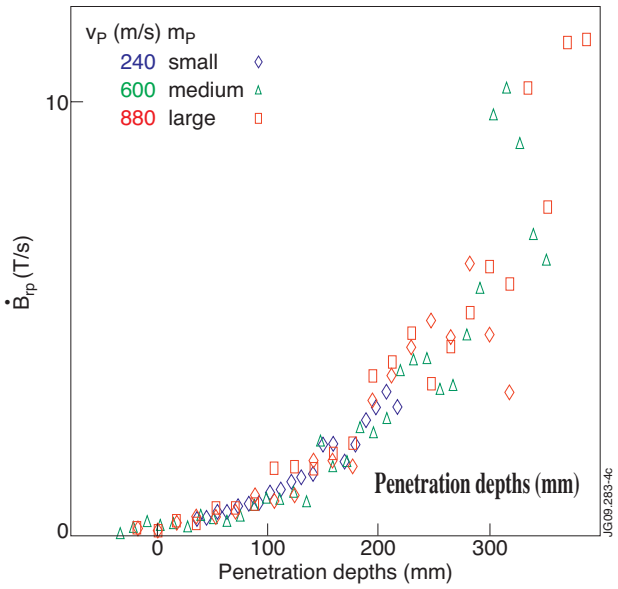

Figure 4: Pellet induced MHD perturbation <B_{rp}> versus pellet penetration along the injection path beyond the separatrix. Different pellet speed and mass result in different penetration depth but do not alter the generated impact (inserted legend, Pulse No's: 22243 small 240m/s; 22559 medium 600m/s; 22310 medium 880m/s; 22537 large 880m/s).

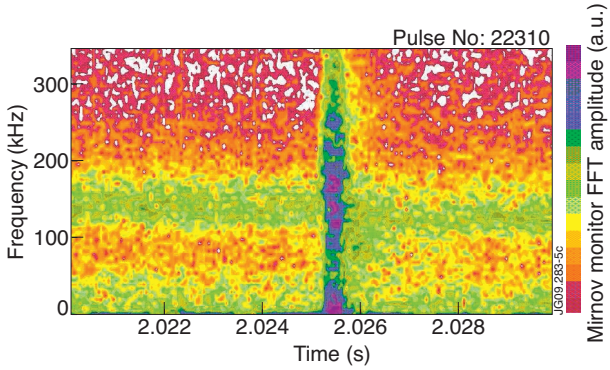

Figure 5: Frequency amplitude evolution derived from a horizontal mid plane LFS Mirnov coil signal. The pellet impact (880m/s example shown in the right part of fig.2) is clearly visible. The broadband intermediate-frequency activity around 150kHz is likely drift Alfvén turbulence driven TAE at the plasma edge in the vicinity of $\rho_{pol} = 0.8$. Present before and after, the pellet just enhances its amplitude transiently by a factor exceeding 100.

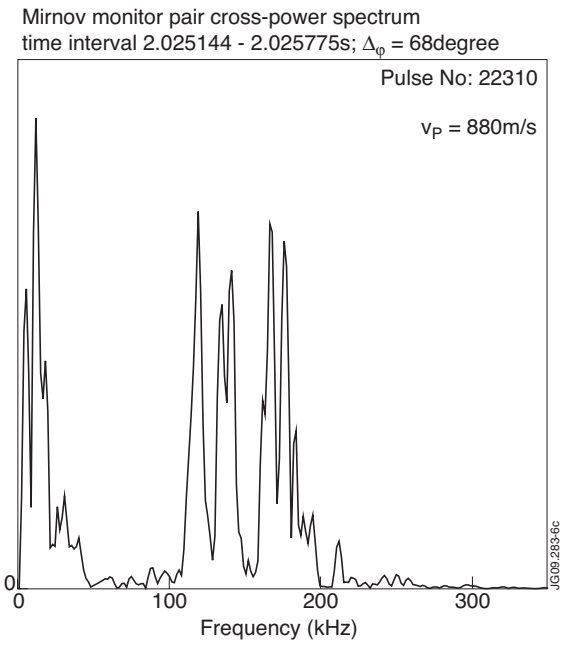

Figure 6: Cross-power spectrum from a Mirnov monitor signal pair [19] located at LFS horizontal mid plane with 68^o toroidal distance. The obvious correlation in both frequency ranges of strong MHD activity is evidence for a coherent mode.

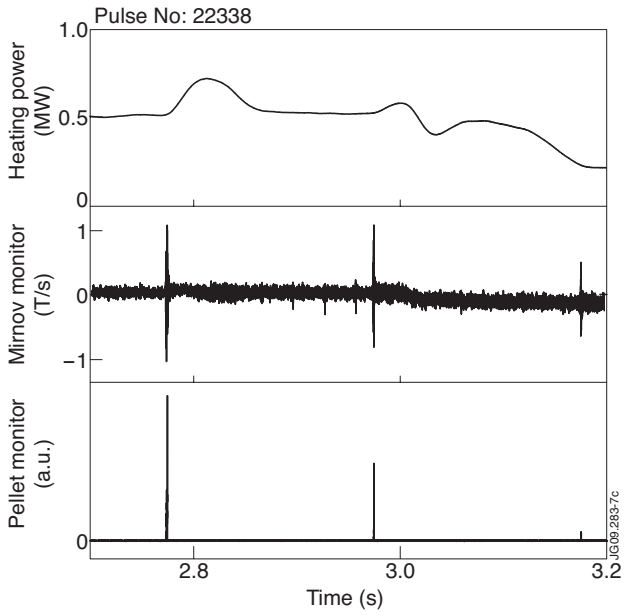

Figure 7: Train of three identical pellets (small 240m/s) injected during the L-mode power ramp down phase before discharge termination. Although subsequent pellets penetrate deeper, the resulting MHD perturbation decreases with heating power. The transient impact of the pellets on plasma parameters causes enhanced ohmic heating.

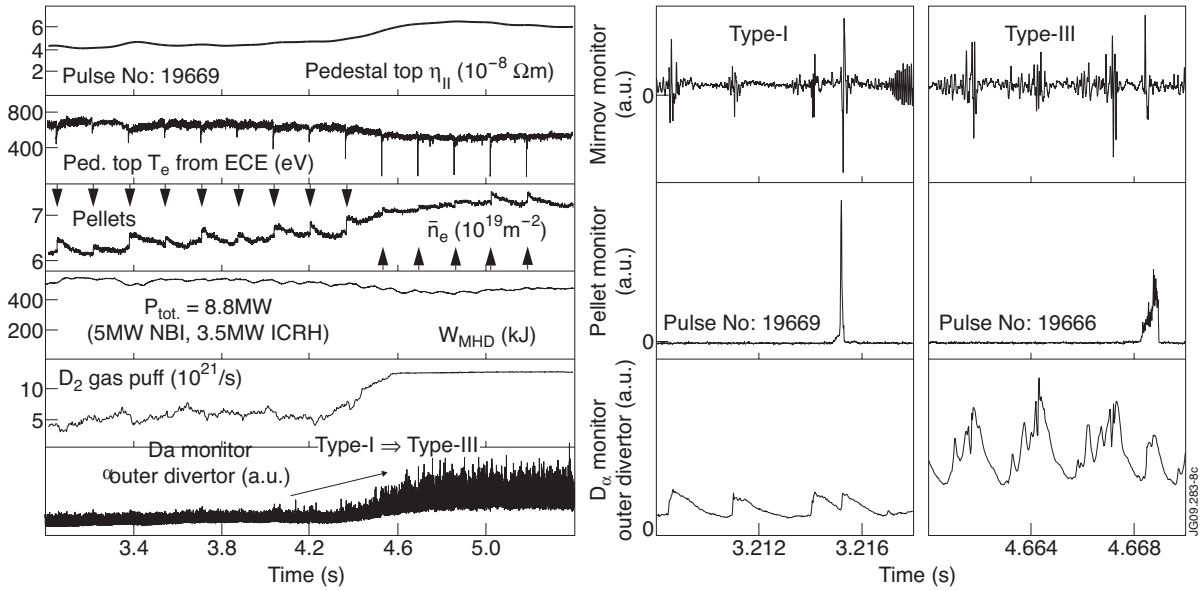

Figure 8: Comparison of spontaneous and triggered ELMs in the type-III regime. A stable type-I H-mode is gradually driven into the type-III regime by the strong gas-puff cooling of the edge and the increase of its resistivity (parallel Spitzer resistivity taking electron data and assuming Z_{eff} = 1)(left). While in the type-III regime spontaneous ELMs typically display a precursor phase and a slow growth, triggered ones evolve much faster by skipping the precursor activity (expanded time scale on far right, data from virtually identical twin shot). They appear more alike to fast growing triggered and spontaneous ELMs in the type-I regime (center).

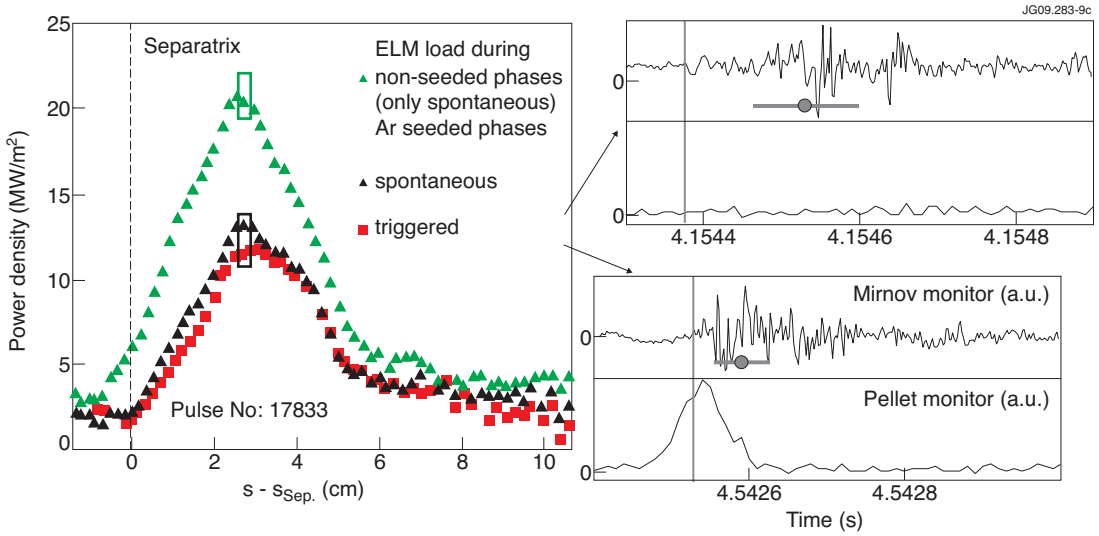

Figure 9: Comparison of spontaneous and triggered type-I ELMs in radiatively cooled edge phases. Whereas there is no di erence in their global action like e.g. the imposed heat load (left) the onset dynamics as characterised by the mode amplitude (right) is different. Pellet triggered events show significantly faster growth to maximum amplitude (60±36μs for the entire sample as indicated) than their spontaneous counterparts (154±68μs). This restores the fast ELM growth typical for the hot edge type-I regime. The Ar seeding results in a significant heat flux reduction on the divertor (left, boxes representing standard deviation of entire sample of events).

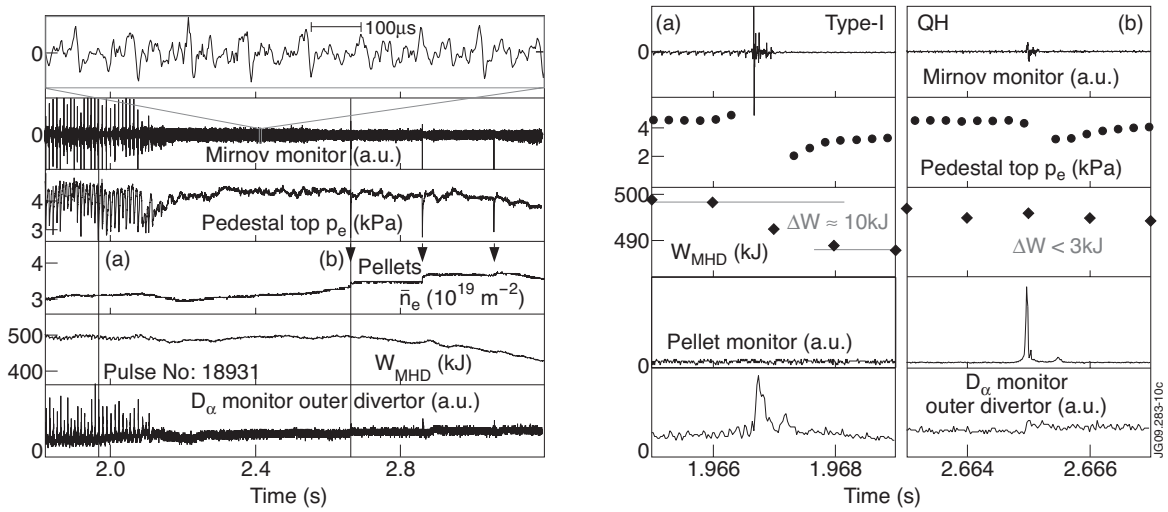

*Figure 10: Pellet injection into QH mode phases does not result in the triggering of an ELM like event. Left: a discharge in which the transition from the type-I ELM regime into a QH phase is achieved while keeping plasma parameters virtually identical. In the course of this transition, burst-like ELM events are replaced by EHOs at about 10kHz, typical for the QH mode (blow-up on top). A pellet injected during the QH phase (right, indicated by **B** in the left part) does not trigger MHD activity similar to a type-I ELM (middle, **A**). Furthermore, no significant energy loss is found as expected in the case of triggering.*

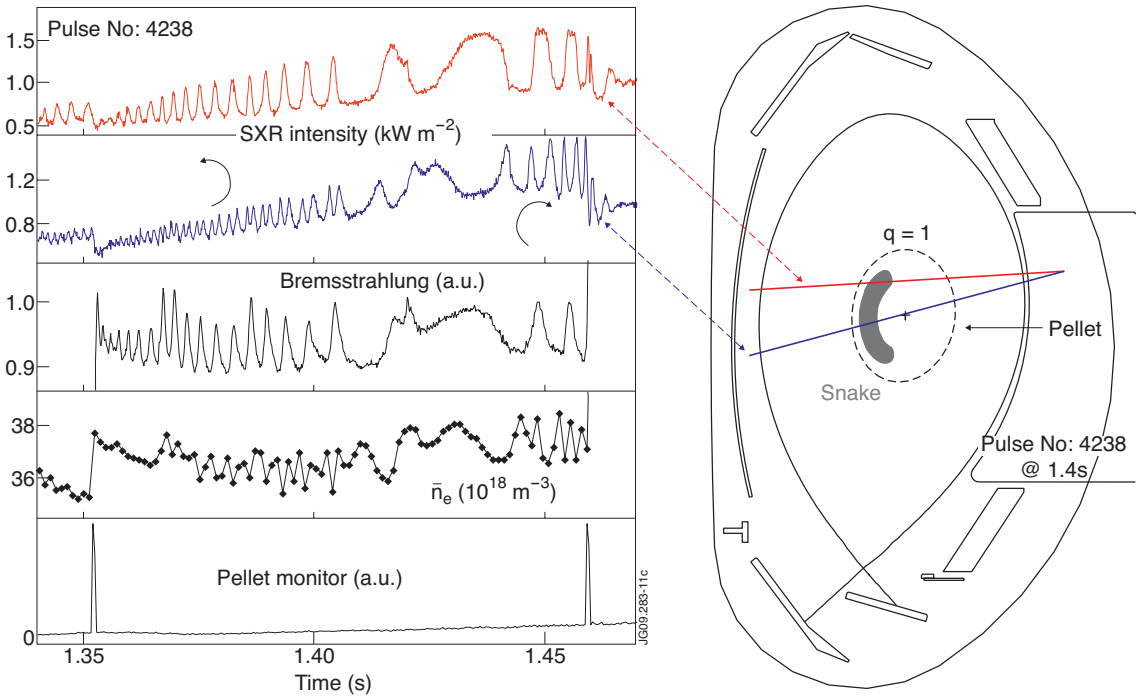

Figure 11: Evolution of a local density enhancement with m=n=1 topology following deep pellet penetration into a OH plasma. This snake carries nally about 0.5% of the plasma and 5% of the injected pellet mass and has a size of approximately 10×30cm.